Image Denoising of Low-Electron-Dose Transmission Electron Microscopy

Zewen Zhang
Stanford University
Stanford, CA
zwzhang@stanford.edu

Abstract

Atomic resolution images of weakly-bonded and reactive materials with transmission electron microscopy (TEM) necessitates lower electron dose and short acquisition time to avoid beam damage. However, lowering the electron dose results in noisy micrographs. In this paper, we first analyze the noise pattern of low-electron-dose images at different total doses, and further explore and compare the denoising methods for low-electron-dose images. We find that at low electron doses below 5 $e^-/Å^2$, the noise can be described with Poisson distributions, while for electron dose above 25 $e^-/Å^2$, the noise follows a Gaussian distribution. Simple spatial filters used in traditional TEM denoise, such as median filters, Weiner filters, Gaussian filters, and non-local detection-based methods, such as non-local means (NLM) and its variants were explored on both simulated noisy images and real low-electron-dose image. We find that block-matching and 3D filtering (BM3D) outperforms other methods in both simulated and real noisy TEM images, however there might be unrealistic features generated. The tradeoff between denoise and unrealistic feature should be balanced.

1. Introduction

High-resolution TEM (HRTEM) enables structural analysis of condensed matters at sub-angstrom resolution. The high spatial resolution characterization is especially critical to the understanding of structure-property relationship in materials science. Nowadays, electron microscopies are widely equipped with CCD cameras. Typical HRTEM micrographs taken with a CCD camera need an electron dose over 10^4 $e^-/Å^2$. Recently, the development of scientific CMOS detectors for TEM, also known as the direct-electron detectors (DEDs), has made possible HRTEM imaging with much less electrons. At the same electron dose, images taken with DED has much better signal-to-noise (SNR) ratios compared to images from CCD cameras. However, electron microscopy study of weakly bonded or reactive materials, such as organic-inorganic hybrid perovskite and metal organic framework, remain difficult by their rapid structural degradation under intense electron beam. The critical dose of these materials, defined as the maximum electron dose before distinct structural change, can be only few to tens of $e^-/Å^2$. Such low electron dose significantly decreases the SNR of the acquired micrographs despite taken DEDs, degrading the quality or even completely prohibiting the extraction of desired critical information from the noisy images. Therefore, it is important to understand the noise characteristics in these low-electron-dose images and develop efficient noise reduction methods.

There are several important sources of noise in a TEM micrograph: (i) quantum noise (shot-noise) of electron beam; (ii) dark current noise from thermally generated electrons; (iii) read-out noise from electronic devices to read the image[1]. The Poisson statistics would apply for the first two sources of noise, whereas Gaussian for the read-out noise. The dark current noise and the read-out noise are independent of beam intensity. The shot noise is proportional to the square root of the number of recorded electrons per pixel.

The noise in TEM images can be described by a Poisson distribution, a Gaussian distribution, or a mixed of both, depending on the electron dose. At low to moderate electron dose, the shot-noise tends to dominate in an electron micrograph. As the electron dose increase, the shot-noise can be treated with an approximate Gaussian distribution. We need to understand the noise pattern for the DED camera at the dose rate for better denoise algorithm design.

Generally, noise reduction algorithms in TEM micrograph can be categorized into two groups, spatial filtering, and temporal filtering. One simple and commonly deployed temporal filtering method is frame averaging. It is important to do motion correction before averaging to account for drift of the samples between frames. Many state-of-the-art software for TEM imaging has automatic drift correction embedded. Therefore, we will mainly focus on spatial filtering methods here.

2. Related Work

2.1. Simple Spatial Filters

Denoising in TEM for materials science is often accomplished by simple spatial filters like Average Background Subtraction filter[2], Wiener filter[3], Gaussian filter[4], or their combinations. These methods are often employed for images from materials robust enough to survive high electron dose to obtain high spatial oversampling. Additionally, the design purpose of these filters for traditional HRTEM images is to distinguish amorphous background and crystalline materials.

2.2. Non-Local Means

Non-local means (NLM) algorithm for image denoising has shown very promising results in both detail preservation and noise removal[5]. Considering the periodicity in the TEM images for materials science, it would have natural advantage for image denoising. The estimated denoised value of a pixel block *u(i)* is computed as a weighted average of a given neighboring pixel blocks *v(j)* in a given search window *S*.

$$u(i) = \frac{1}{Z(i)} \sum_{j \in S} e^{-\frac{\sum(v(j)-u(j))^2}{h^2}} v(j)$$

The intuition behind NLM filter is that any image has a degree of redundancy, and a pixel of the image may have similar pixels which are beyond its spatial neighborhood. In this approach, the noisy pixel-values are replaced by a weighted average of all pixels in a large patch of the image, where the weights are determined by the neighborhood similarity of the pixel-pairs.

2.3. Block-matching and 3D filtering (BM3D)

By replacing the weighted average of intensities of pixels with similar neighborhoods in a given search window by more advanced collaborative filtering, BM3D algorithm is one of the most successful variants in non-local detection-based methods, and are suitable for images with structural redundancy[6].

3. Methods

3.1. Image Preparation

For noise pattern analysis, flat field images were taken over vacuum under uniform electron beam illumination with Thermo Fisher Titan 80-300 kV ETEM equipped with a Gatan K3IS DED camera in the electron-counting mode with the dose fractionation function. The image was taken with various total doses from 1 $e^-/Å^2$ to 30 $e^-/Å^2$. Five subframes were summed together after auto motion correction.

Since we cannot have ground truth image for real low electron dose images, we will need to simulate noisy TEM images from "noiseless" images for method evaluation. Here, we use HRTEM image of crystalline silicon taken with high electron dose of over 10^4 $e^-/Å^2$ as the ground truth

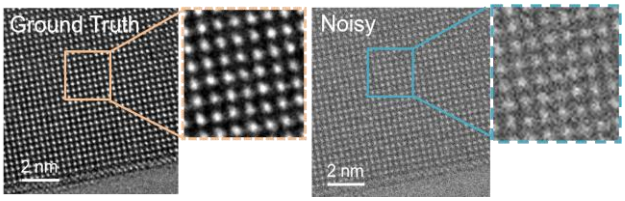

Figure 1: Ground truth image of crystalline silicon and simulated noisy TEM images.

(Figure 1). And after analyzing the noise pattern, we blur the image with a Gaussian kernel of and add random Gaussian noise to the image to simulate low-electron-dose images (Figure 1). We deliberately make the simulated image less noisy than real low-electron-dose image to evaluate these methods, otherwise we cannot tell the difference between these methods.

The sample for real low-electron-dose image was hybrid halide perovskite nanowire. The image was taken Thermo Fisher Tecnai F20 TEM equipped with a Gatan K2 DED camera in the electron-counting mode with the dose fractionation function. The image was taken with 12 $e^-/Å^2$ Five subframes were summed together after auto motion

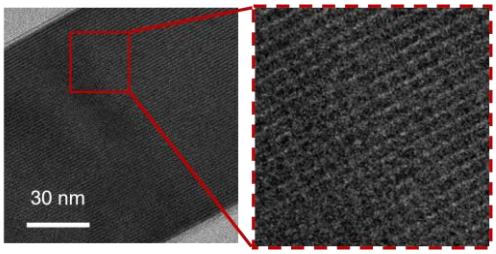

Figure 2: Low-electron-dose image of hybrid halide perovskite.

correction.

3.2. Denoise Algorithm

Considering the high noise level in the low-dose-image, we implemented a locally adaptive non-local means (LANLM) method to be better handle the noise

characteristics in the image[7]. Specifically, we will have a threshold for the parameter *h* to avoid extreme situations.

$$h = \begin{cases} \beta t_u \sigma_I, & \sigma_N \ll t_u \sigma_I \\ \beta t_l \sigma_I, & \sigma_N \gg t_u \sigma_I \\ \beta \sigma_N, & otherwise \end{cases}$$

β is the filtering parameter which controls the degree of filtering which we set it to be 10, and σ_N is the standard deviation of the local neighborhood, and σ_I is the standard deviation of the entire image, respectively. The constants t_u = 0.7 and t_l = 1.2 are used as the threshold to avoid some extreme situations when the local standard deviation is too small or too large.

3.3. Evaluation Metrics

We use higher peak signal-to-noise ratio (PSNR) value and structural similarity index measure (SSIM) as quantitative evaluation metrics for image denoising.

$$\text{MSE} = \frac{1}{mn} \cdot \sum_{i=0}^{m-1} \sum_{j=0}^{n-1} (I(i,j) - K(i,j))$$

$$\text{PSNR} = 10 \cdot \log_{10} \left(\frac{MAX^2}{MSE}\right)$$

I denotes the noise-free image with a dimension of *n* x *m*, K denotes the noisy image. MAX is the maximum possible pixel value of the image, MSE is calculated as above.

$$\text{SSIM} = \frac{(2\mu_I\mu_K + c_1)(2\sigma_{IK} + c_2)}{(\mu_K^2 + \mu_I^2 + c_1)(\sigma_K^2 + \sigma_I^2 + c_2)}$$

μ is the average of an image, σ is the variance of an image, σ_{IK} is the covariance of I and K. c_1 is $(0.01L)^2$, c_2 is $(0.03L)^2$, where L is the dynamic range of the pixel value.

We will also qualitatively evaluate the image with our prior knowledge on the crystal structure of target materials. Since PSNR and SSIM are designed for natural images, while TEM images have different properties.

4. Results and Discussion

4.1. Noise Pattern Analysis

From Figure 3, we can see at extremely low electron dose condition, around 1 $e^-/Å^2$, the pixel intensities are discretized into four regions. This is because the DED is working in electron counting mode, where the arrival of single electron could be detected. This distribution corresponds to a Poisson process. For electron dose below 5 $e^-/Å^2$, the histograms of pixel intensities all look discretized

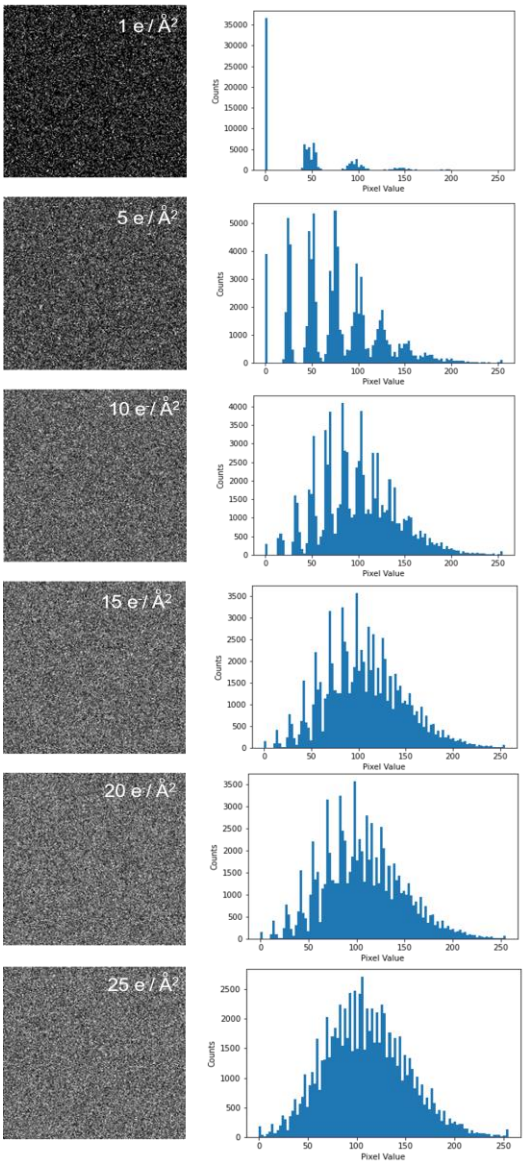

Figure 3: Low-electron-dose flat field images taken at different total doses with corresponding histograms of pixel intensities. The images are 170 × 170 pixels.

and follow Poisson distributions, albeit a peak shift to a higher average intensity. For electron dose 25 $e^-/Å^2$, the pixel intensities become more of a Gaussian distribution. In between 5 $e^-/Å^2$ to 25 $e^-/Å^2$, the distribution seems to a mixture of Gaussian and Poisson process. Notably, in traditional HRTEM imaging, the total dose is well above the value discussed here, as a result the filters are designed to deal with Gaussian noises. In the low-electron-dose regime, different noise models should be considered.

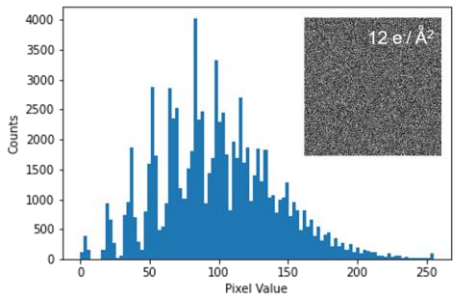

Figure 4: Flat field image and corresponding pixel intensity histograms taken at a total dose of 12 $e^-/Å^2$.

4.2. Simulated Noisy Image Denoising

The target low-electron-dose image was taken at a total dose of 12 $e^-/Å^2$. Based on the pixel intensity histogram of the flat field image taken at similar total dose (Figure 4), the noise should be best described as a mixture of Poisson and Gaussian distribution but could be approximated as a Gaussian process. Therefore, for simplicity, the simulated image was blurred with a Gaussian kernel with standard deviation of 0.8 and random Gaussian noise. The image was then subsampled by a factor of 2. As shown in Figure 1, the ground truth image shows clear atom columns of crystalline silicon. The simulated image also shows Si atomic columns, but the center of each column is not clear anymore.

Next, we experimented with all the filtering methods described in the Section 3 on the simulated noisy image. The results are shown in Figure 5. Briefly, all denoised images have higher PSNR values compared to simulated noisy image (Table 1). Weiner filtered image shows better performance than Gaussian and Median filters. Among these methods, BM3D gives the highest PSNR of 19.86 dB, outperforming all other methods. Similar trend can be seen in SSIM (Table 2). This matches well the fact that TEM images of crystalline materials feature in their periodicity. The self-similarities in neighboring pixel blocks give natural advantages to these non-local detection methods.

However, we also notice that our own version of NLM and LANLM do not work as well, although LANLM did show a slight improvement over NLM. We have experimented with different searching window size, from 7 × 7 pixels to 35 × 35 pixels. Nonetheless, the denoised images do not show much improved quality as expected. We hypothesize that this is because the size of repetitive feature in the image is too large. Here each atomic column is around 11 × 11 pixels, only around 8 similar blocks can be found in our largest search window, and the image is highly noisy, therefore the denoising effect will be limited. Since our own implementation of these methods are not optimized for computation efficiency, we did not further expand the searching window to verify our hypothesis.

Notably, TV prior denoising method showed second best performance in terms of PSNR and SSIM, however the image looks patchy, which is impossible for a real TEM image. TV prior is designed for natural images which might not work for TEM images. Further analysis of TEM image will be needed to best describe the feature and figure out a better prior.

Additionally, it is also important to point out that BM3D filtered image have some distortion at the edge. The atom columns seem distorted compared to the ground truth image. Although the center positions remain unaltered, this could still raise some concerns. Unlike natural images where the visual effect matters. For TEM images, the accurate determination of atom and lattice positions matter because correct quantification of these key parameters will be meaningful to understand materials properties.

Noisy	Gaussian	Median	Weiner
13.05	16.62	14.45	16.38
ADMM+TV	NLM	LANLM	BM3D
18.99	14.31	14.23	19.86

Table 1: PSNR of simulated noisy and denoised images, units dB.

Noisy	Gaussian	Median	Weiner
0.54	0.78	0.66	0.72
ADMM+TV	NLM	LANLM	BM3D
0.72	0.56	0.59	0.85

Table 2: SSIM of simulated noisy and denoised.

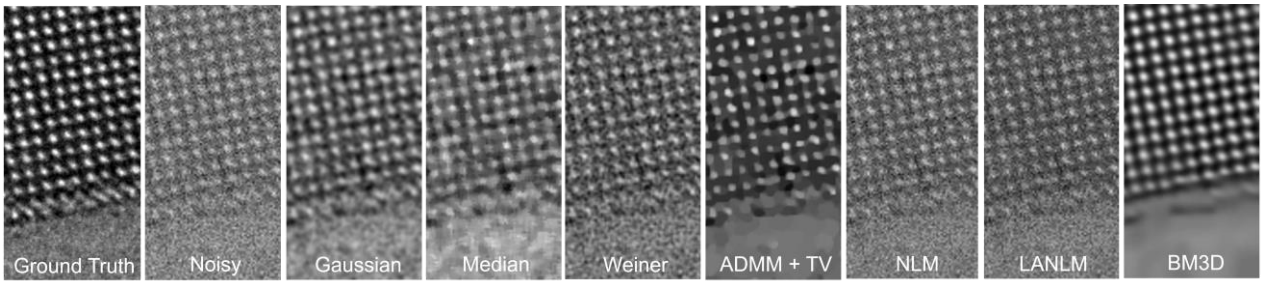

Figure 5: Ground truth image, simulated noisy image, and denoised images of crystalline silicon.

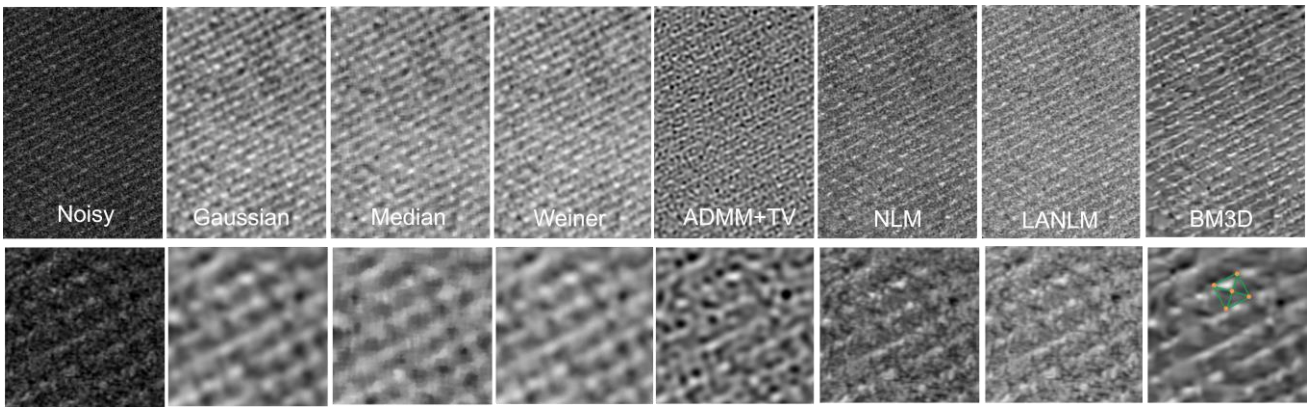

Figure 6: Real low-electron-dose image and denoised images of hybrid halide perovskite.

4.3. Real Low-Electron-Dose Image Denoising

For real low-electron-dose denoising, the image is noisier than simulated. The features, atom columns or lattices, are hardly distinguishable from the background. Since we do not have prior knowledge on the noise distribution, such as standard deviation, we had to experiment with different values to get relatively better results. As a note here, we can not use the noise distribution from the flat field image with similar total dose, because the total dose is calculated based on the time and electron dose rate used which is calibrated over vacuum. However, samples will deflect electrons. Heavier elements and thicker samples will deflect electrons more, therefore the real electron dose over this area is not known.

The filtered images are shown in Figure 6 along with the raw image. Since we do not have a ground truth image, we will evaluate the result based on our prior knowledge on the crystal structure and visual effect.

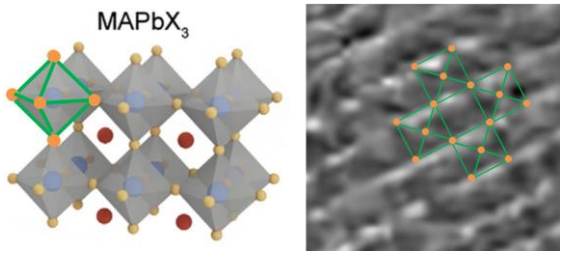

Figure 7: Schematic of hybrid halide perovskite crystal structure and zoomed-in image of BM3D filtered image.

Qualitatively, BM3D gave the best result among these methods. The lattices can be clearly observed in BM3D filtered image, while vague or disappeared in other filtered images. We can distinguish some square patterns in the filtered image, which is in good agreement with the crystal structure of hybrid halide perovskite. Notably, in BM3D filtered image, we can even distinguish the pyramid-like structure in the perovskite lattice, as shown in Figure 7. The pyramid structure is highlighted with green lines and orange dots. Simple spatial filters, Gaussian and Weiner filters have slightly better effect than Median filter, but they both look blurry. TV denoising method completely wash away the information in the image due to the incorrect assumption about TEM image features. NLM and LANLM still did not work well due to the reason discussed above.

4.4. Future Work

It is important to note that the denoising methods we explored here are designed for Gaussian noise removal. However, a mixed Poisson and Gaussian model would be a better approximation of the noise pattern. These methods could be tailored to better account for the mixed noise pattern.

Furthermore, for materials that are more sensitive than hybrid halide perovskite, whose critical dose might be below 5 $e^-/Å^2$, the noise will be better described with a Poisson distribution. Variants of these denoising methods should be developed and evaluated.

5. Conclusion

In summary, we investigated the noise patterns in TEM images taken at low electron doses from 1 $e^-/Å^2$ to 25 $e^-/Å^2$. We find that the noise pattern can be best described as a Poisson distribution at a total dose lower than 5 $e^-/Å^2$, while for images with a total dose higher than 25 $e^-/Å^2$, the noise will follow a Gaussian distribution. In between, the distribution needs to be described as a mixture of both.

Based on the above analysis, we explored and evaluated simple spatial filtering methods commonly used in traditional HRTEM and non-local detection-based methods on both simulated noisy images and real low-electron-dose image. Among these methods, non-local detection-based methods, BM3D gave the best denoised image, with

highest PSNR and SSIM, while maintaining the fine details of the image.

References

[1] H. Du, “A nonlinear filtering algorithm for denoising HR(S)TEM micrographs,” *Ultramicroscopy*, vol. 151, pp. 62–67, Apr. 2015.

[2] R. Kilaas, “Optimal and near-optimal filters in high-resolution electron microscopy,” *J. Microsc.*, vol. 190, no. 1–2, pp. 45–51, 1998.

[3] L. D. Marks, “Wiener-filter enhancement of noisy HREM images,” *Ultramicroscopy*, vol. 62, no. 1, pp. 43–52, Jan. 1996.

[4] A. F. De Jong, W. Coene, and D. Van Dyck, “Image processing of HRTEM images with non-periodic features,” *Ultramicroscopy*, vol. 27, no. 1, pp. 53–65, Jan. 1989.

[5] A. Buades, B. Coll, and J.- Morel, “A non-local algorithm for image denoising,” in *2005 IEEE Computer Society Conference on Computer Vision and Pattern Recognition (CVPR’05)*, Jun. 2005, vol. 2, pp. 60–65 vol. 2.

[6] K. Dabov, A. Foi, V. Katkovnik, and K. Egiazarian, “Image Denoising by Sparse 3-D Transform-Domain Collaborative Filtering,” *IEEE Trans. Image Process.*, vol. 16, no. 8, pp. 2080–2095, Aug. 2007.

[7] D.-Y. Wei and C.-C. Yin, “An optimized locally adaptive non-local means denoising filter for cryo-electron microscopy data,” *J. Struct. Biol.*, vol. 172, no. 3, pp. 211–218, Dec. 2010.